JOURNAL OF CHEMICAL INFORMATION AND MODELING

Article

pubs.acs.org/jcim

Homology Models of Human All-Trans Retinoic Acid Metabolizing Enzymes CYP26B1 and CYP26B1 Spliced Variant

Patricia Saenz-Méndez,[†] Ali Ateia Elmabsout,[‡] Helena Sävenstrand,[§] Mohamed Khalid Alhaj Awadalla,[‡] Åke Strid,[§] Allan Sirsjö,[‡] and Leif A. Eriksson*[,∥]

[†]Computational Chemistry and Biology Group, Facultad de Química, UdelaR, 11800 Montevideo, Uruguay

[‡]Department of Clinical Medicine, School of Health Sciences, Örebro University, SE-701 82, Örebro, Sweden

[§]Department of Science and Technology, Örebro Life Science Center, Örebro University, SE-701 82, Örebro, Sweden

[∥]Department of Chemistry and Molecular Biology, University of Gothenburg, 412 96 Göteborg, Sweden

Supporting Information

ABSTRACT: Homology models of CYP26B1 (cytochrome P450RAI2) and CYP26B1 spliced variant were derived using the crystal structure of cyanobacterial CYP120A1 as template for the model building. The quality of the homology models generated were carefully evaluated, and the natural substrate all-*trans*-retinoic acid (atRA), several tetralone-derived retinoic acid metabolizing blocking agents (RAMBAs), and a well-known potent inhibitor of CYP26B1 (R115866) were docked into the homology model of full-length cytochrome P450 26B1. The results show that in the model of the full-length CYP26B1, the protein is capable of distinguishing between the natural substrate (atRA), R115866, and the tetralone derivatives. The spliced variant of CYP26B1 model displays a reduced affinity for atRA compared to the full-length enzyme, in accordance with recently described experimental information.

INTRODUCTION

Retinoic acid (RA), the most active metabolite of dietary vitamin A (retinol, ROH), is an essential regulator of gene expression and an important factor in regulation of cell proliferation and differentiation.[1,2] Biologically active retinoid metabolites are synthesized in the target cells, with the leading source for this synthesis being all-trans retinol (atROH) taken up from the plasma.[3] Vitamin A is converted to retinaldehyde and then further to all-trans retinoic acid (atRA) by two oxidation steps involving different alcohol dehydrogenases and retinaldehyde dehydrogenases. The latter process is believed to be the rate-limiting step in the biosynthesis of atRA. Once formed, atRA is either converted to less active polar metabolites or attached to nuclear hormone receptors.[4] Retinoid signaling through retinoic acid receptors is crucial for regulation of several cellular processes such as differentiation, migration, and proliferation.[5] The cytochrome P450 (CYP) superfamily of heme-binding monooxygenases catalyzes a large number of biological reactions, such as oxidative conversion of many steroids, xenobiotics, and environmental toxins. This large superfamily consists of at least 74 families each with notable functions in mammalian species.[6] Most CYPs are associated with microsomal membranes and generally expressed in the liver. There are several microsomal CYPs, such as CYP1A1, CYP4A11, CYP3A4/5/7, and CYP2C8/9, which are suggested to be involved in retinoid metabolism.[7] However, CYP26 is apparently the most important enzyme responsible for catabolism of retinoic acid. It regulates intracellular levels of retinoids and degrades them into inactive derivatives or polar metabolites such as 4-oxo-RA, 4-OH-RA, 5,6-epoxy-RA, and 18-OH-RA.[8−11]

CYP26 recognizes RA as its substrate, and the expression or activity of this isozyme can be induced by RA both in vitro and in vivo.[6,12,13] Three isoforms of CYP26 are present in humans: CYP26A1, CYP26B1, and CYP26C1.[6] Studies on substrate specificity show that CYP26A1 and CYP26B1 are specific for atRA, whereas CYP26C1 efficiently metabolizes both atRA and 9-*cis*-RA.[9,14,15] The phenomenon of retinoic-acid resistance during treatment of hematopoietic leukemia[16] may be a consequence of an accelerated retinoid catabolism induced by CYP26 enzymes.[17−19] Thus, inhibition of CYP26 by retinoic acid metabolism blocking agents (RAMBAs) increases both plasma and tissue levels of atRA and enables the desired retinoidal effects.[20]

The CYP26B1 gene covers about 18 000 base pairs (bp) divided into six exons and a large second intron of 8.57 kb.[21,22] The gene also has a long untranslated 3′ region of almost 3 kb. Recently, the function of a spliced variant of this gene, lacking exon 2, has been reported (Figure S1, Supporting Information).[23] In this work, the authors described that the spliced variant shows a slower and reduced degradation of atRA,

Received: June 11, 2012
Published: September 18, 2012

suggesting that this enzyme regulates the rate of atRA degradation. Considering that the interaction of CYP26B1 spliced variant with cofactors and other proteins is unknown and that the enzyme may play a key role in the regulation of intracellular levels of retinoids, the need for further studies on its substrate specificity becomes clear.

Although the amino acid sequence of CYP26B1 is known, no crystal structure is available. This makes a detailed analysis of the metabolic degradation of atRA difficult and therefore also the rational design of RAMBAs. It is thus essential to determine the 3D structure employing different approaches, such as homology modeling, assuming that the tertiary structure and folding of two proteins are similar if the sequences are related.[24] Homology models of CYP26A1 and CYP26B1 have been described previously.[25,26]

To this end, we previously employed two different approaches for building initial models of the spliced variant of CYP26B1. One potential structure was obtained simply by deleting exon 2 from the available full-length homology model of CYP26B1.[26] In addition, a homology model was created using the same CYP26B1 model as template. However, the heme group could not be placed into the model, even though in theory it would be possible to insert this moiety since we observed that some amino acids responsible for the binding and orientation of the heme were still intact. Hence, the problem was rather related to the surrounding residues that made the binding pocket too tight for the heme to fit in the spliced homology model.

These results prompted us to redesign our models of both full-length and spliced variant of CYP26B1. For CYP26B1, the current study represents an improved and refined model, whereas for the spliced variant this is the first model described in the literature so far.

THEORETICAL CALCULATIONS

Computational Approaches. All molecular modeling was performed using the YASARA program.[27,28] All structures of ligands, CYP26B1, spliced CYP26B1, and enzymes in complex with ligands were geometry minimized using the AMBER03[29] molecular mechanics force field to within an rms gradient of 0.1 kcal mol^{-1} $Å^{-1}$. All systems were immersed in a box of water molecules whereafter simulated annealing minimization was performed. Solvated systems were neutralized by adding sodium and chloride ions in random locations. Protonation states were assigned taking into account pK_a values and simulation pH 7. To obtain relaxed geometries, a short (5 ns) molecular dynamics (MD) simulation was performed and followed by a final energy minimization step. MD simulations on all models were performed using the canonical NVT ensemble at 298 K and using periodic boundary conditions. Long-range electrostatic energies were calculated using the particle mesh Ewald (PME) method.[30] Simulations were carried out with multiple time steps, namely, 1.25 fs for intramolecular forces and 2.5 fs for intermolecular ones. MD trajectories were sampled every 5 ps, resulting in 1000 snapshots per simulation.

Model Building. The protein sequence of human CYP26B1 was obtained from the NCBI server (no. 9845285). Following our previous report,[26] homology models for this enzyme were built using the crystal structures of the human CYP2C8 (PDB code 1PQ2), CYP2C9 (PDB code 1OG2), and CYP3A4 (PDB code 1TQN) as templates. The sequence similarity between CYP26B1 and the three template structures was 26%, 22%, and 24%, respectively. Using these three templates, multiple sequence alignment and models were obtained. Even though human CYP2C8 shows the best sequence identity, the fit is quite low and may not fall into the "safe" homology region. Considering the fact that the higher the percentage of identical residues the better the model, we used the sequence of CYP26B1 to search for other templates not considered until now, employing BLAST.[31] Retinoic acid-binding cyanobacterial CYP120A1 (PDB code 2VE3)[32] displayed the highest sequence identity (34%). Such a percentage of sequence identity is within the limit for obtaining reasonably good models, and if the subsequent structural assessment shows good quality, the model may be considered as reliable.[33] Indeed, a protein with sequence identity over 30% can be predicted with an accuracy comparable to a low- to medium-resolution X-ray structure.[34] Albeit the template is not of mammalian origin, it has been shown that CYPs in eukaryotic and prokaryotic organisms share similar 3D structures and folding patterns.[35] This reinforced the idea of employing this enzyme as a template for homology modeling of CYP26B1.

Model Validation. The final models were evaluated employing different programs, such as Procheck, Verify 3D, and the RAMPAGE server, which allow checking the stereochemical quality of the models and calculation of the percentage of conformations in favored regions obtained from Ramachandran plots.[36−38]

Docking. Ligands were docked into the active site of the homology models using YASARA, which includes an integrated version of AutoDock[39] with a Lamarckian genetic algorithm. A 30 × 30 × 30 point grid with a spacing of 0.375 Å centered at the heme group iron atom was employed. In the docking studies, flexible ligand structures were generated. A total of 25 separate docking runs were performed in each case, and the lowest energy structure from each run was retained. Final docked conformations were classified in clusters using a rmsd of 5 Å. The cluster with the best preliminary binding energy was then selected.

Energy Calculations of the Enzyme−Ligand Complex. Besides the binding energy recorded by Autodock (results not shown), the results were improved by calculating the binding energy in YASARA. The binding energy was obtained by calculating the energy at infinite separation of the ligand (unbound state) and subtracting the energy of the enzyme−ligand complex (the bound state). A more positive binding energy is defined herein as a more favorable interaction for a given force field. All involved structures were subjected to MD simulation and minimization prior to calculation of binding energies.

RESULTS AND DISCUSSION

Homology Model of CYP26B1. It has been described that of the P450 enzymes responsible for 4-hydroxylation of atRA in the human liver, CYP2C8 is a major contributor, as well as CYP3A4 and CYP2C9,[8] among others. On the basis of this observation, previous homology models for CYP26B1 have been derived employing those enzymes as templates.[25,26] In this work, the amino acid sequence of human CYP26B1 (no. 9845285) was used to search for new templates using BLAST. The BLAST search results as well as the Z score after the corresponding homology modeling are shown in Table 1.

The hybrid template model was built using CYP2C8, CYP2C9, and CYP3A4 as multiple templates and merging

Table 1. Cytochrome P450 Proteins Used As Templates: Sequence Similarity According to BLAST and Z Score Calculated in YASARA after Homology Modeling

template	PDB code	% sequence similarity	Z score
CYP2C8	1PQ2	26	−1.822
CYP2C9	1OG2	22	−2.149
CYP3A4	1TQN	24	−1.898
hybrid template			−1.767
CYP120A1	2VE3	34	−0.627

the best parts of each model into one. Accuracy was slightly increased as the resulting model presents a higher Z-score difference value after homology modeling than models developed from CYP2C8, CYP2C9, or CYP3A4 as sole templates. The Z-score difference value for a pair of structures represents the number of standard deviations by which their similarity exceeds the mean of the distribution of a comparison of similarity among a set of structurally unrelated proteins. Close to zero Z scores increase the probability that two proteins have a common evolutionary origin.[40]

These results clearly showed that the best model was derived using a nonmammalian enzyme as template. Even though all homology models were refined and analyzed, considering the novelty and improved quality of the CYP26B1 model derived from CYP120A1, further studies in this work are only related to this particular model. The homology model of CYP26B1 and the best template (CYP120A1) superpose very well, as shown in Figure 1A.

After energy minimization, MD simulation and final energy minimization were performed and the resulting model evaluated. A Ramachandran plot showed that 97.6% of the residues are located in favored regions, meaning that the model has good quality. Verify 3D analysis calculates the compatibility of an atomistic model (3D) with its own amino acid sequence (1D). Negative scores are indicative of potential problems.[41] For comparison, in Figure 2A Verify 3D superposed plots for models obtained with CYP3A4 and CYP120A1 are shown. From the analysis it is clear that the newly derived model presents a better 3D−1D compatibility.

All results are consistent, and it is thus possible to conclude that the new model based on a prokaryotic template is an improved model compared to previously reported ones.

Ligand Docking into CYP26B1. Further evaluation of the homology model of CYP26B1 was performed by docking known inhibitors reported in the literature (Figure 3). Experimental data was obtained from the MCF-7 assay for metabolic inhibition of atRA reported by Yee et al.[42] The presence of CYP26A1 and CYP26B1 has been confirmed, and both enzymes are induced in response to atRA.[43]

First, atRA was docked in the active site of CYP26B1, which positioned the C4 atom positioned 4.93 Å from the heme iron. atRA also presents multiple hydrophobic interactions with the amino acids Trp65, Trp117, Thr121, Leu125, Phe222, and Phe295 (Figure 4A). Hydrogen-bond interactions between the carboxyl group of atRA and both Arg95 and Ser369 anchor the molecule within the active site.

The theoretically calculated binding energies for atRA and the different RAMBAs are shown in Table 2. Tetralones 2 and 5 showed higher binding energies than expected considering the IC50 values, thus resulting in complexes more stable than indicated by the experimental findings. One explanation for this deviation is that the data reported by Yee et al. were obtained on CYP26A1 isoform assays,[42] which thus can be expected to behave slightly differently over CYP26B1.[26] No information on binding to CYP26B1 is available. Another possible explanation can be that the two hydroxyl groups present in tetralone 5 result in increased interaction between the ligand and the enzyme, and for tetralone 2, the methoxy group establishes a very strong hydrogen bond with the N−H group of Ser369.

The most important aspect regarding this work is that the homology model developed is capable of differentiating between the natural substrate (atRA), a strong inhibitor (R115866), and weaker inhibitors. From the validation results the model behaves better than previous reported models in terms of 3D structure and chain stereochemistry, and we therefore conclude that the newly derived model is reliable and suitable to use as a template to derive for the first time a homology model of the spliced variant of CYP26B1.

Homology Model of CYP26B1 Spliced Variant. The homology model of the CYP26B1 spliced variant was created using the full-length CYP26B1 homology model derived in this work as template. The Z-score difference after homology modeling was −1.049, representing an overall satisfactory model. As can be seen in Figure 1B, the homology model of CYP26B1 spliced variant and the full-length template superpose very well.

After energy minimization, MD simulation, and subsequent energy minimization as a final step, the model was validated. The Ramachandran plot indicated that 98.0% of the residues are located in favored regions (Figure S2, Supporting Information). In addition, the Verify 3D plot shows than the

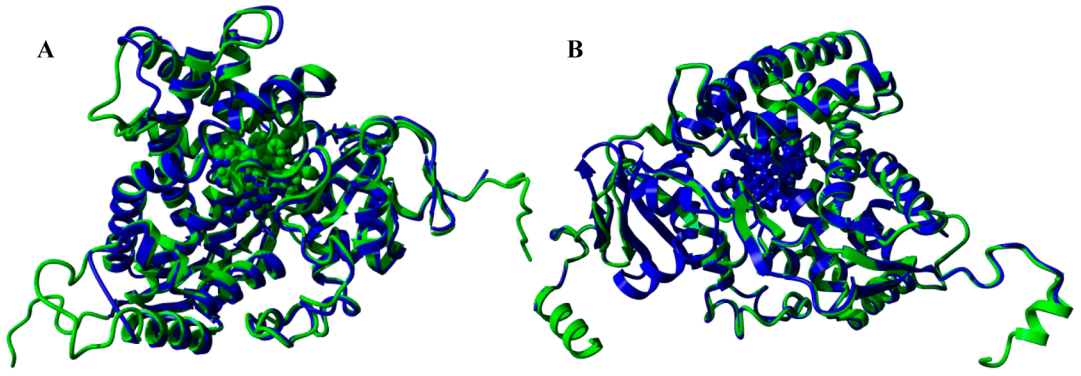

Figure 1. Superposed backbones of homologues: (A) CYP26B1 in green and CYP120A1 (2VE3) in blue; (B) CYP26B1 spliced variant in green and CYP26B1 full length in blue.

dx.doi.org/10.1021/ci300264u | J. Chem. Inf. Model. 2012, 52, 2631−2637

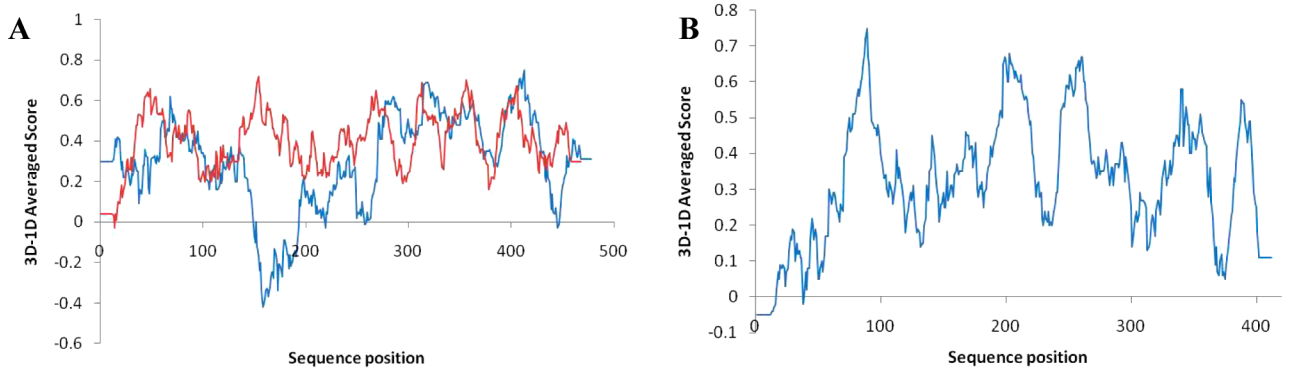

Figure 2. (A) Superposed Verify 3D plots for CYP26B1 homology models: CYP26B1 from template CYP3A4 in blue and from CYP120A1 in red. (B) Verify 3D plot for CYP26B1 spliced-variant homology model.

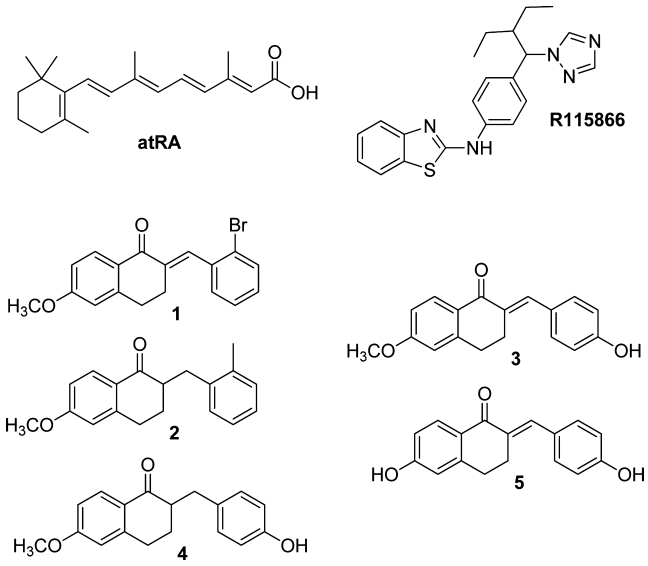

Figure 3. Ligands used for evaluation of docking capabilities in CYP26B1 and CYP26B1 spliced-variant homology models; 1−5 tetralone-derived RAMBAs reported by Yee et al.[42]

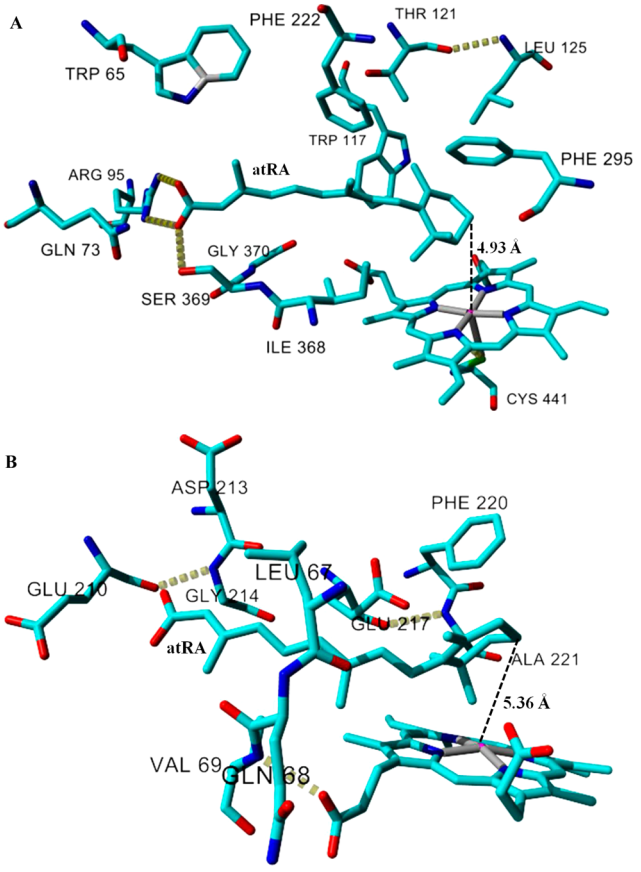

Figure 4. (A) atRA docked in CYP26B1. (B) atRA docked in CYP26B1 spliced variant. Key amino acids and heme group are displayed in stick drawing. Hydrogen bonds are represented as yellow dashed lines.

compatibility of the 3D structure with the amino acid sequence is very satisfactory (Figure 2B).

The heme group is perfectly inserted into the model. Even though deletion of exon 2 in CYP26B1 results in removal of 75 amino acids (Figure 1), the active site is still suitable to hold and retain the heme group.

In full-length CYP26B1, it was observed that the heme group interacted with amino acid residues in the active site through several hydrophobic interactions, including the side chain of residues Trp114, Val130, Leu293, Ala296, Ala297, Thr300, Met362, Ile368, Gly371, Phe434, Gly435, Pro433, and Gly443. The fifth ligand for the iron atom in the heme group is Cys441. The carboxyl side chains in the heme moiety forms hydrogen bonds to His138, Arg142, and Arg373 (Figure 5A). In the CYP26B1 spliced variant, most of these amino acid residues are also present in the active site, interacting with the heme group. Cys366 is the iron binding amino acid, and hydrophobic interactions occur with Gln68, Leu218, Ala221, Ala222, Thr225, Met287, Pro292, Ile293, Gly296, Ile321, Pro358, Phe359, Gly360, Val363, Gly368, and Leu371 (Figure 5B), corresponding to amino acids Gln68, Leu293, Ala296, Ala297, Thr300, Met362, Pro367, Ile368, Gly371, Ile396, Pro433, Phe434, Gly435, Val438, Gly443, and Leu446 using the numbering of the full-length sequence.

Analyzing the two heme binding environments it is clear that most of the residues involved are the same when comparing both active sites (full-length and spliced-variant enzymes). However, in spliced CYP26B1, only Val69 interact with the heme carboxyl side chain through a hydrogen bond. Even though Arg364 is in the active site, its conformation is different when compared to Arg373 in the full-length enzyme. This conformational change hampers hydrogen-bond formation.

At this point, it is possible to conclude that the newly derived spliced-variant homology model, based on our full-length

dx.doi.org/10.1021/ci300264u | J. Chem. Inf. Model. 2012, 52, 2631−2637

Table 2. Binding Energy Calculations from MD-Simulated CYP26B1 Complexes (kcal mol^{-1})

ligand	IC50 (μM)[a]	binding energy
atRA (inducer)		381.12
R115866	0.005	81.71
1	9	54.21
2	30	54.78
3	7	65.73
4	5	78.41
5	9	70.92

[a]Results obtained from MCF-7 CYP26A1 cell assay reported by Yee et al. [42]

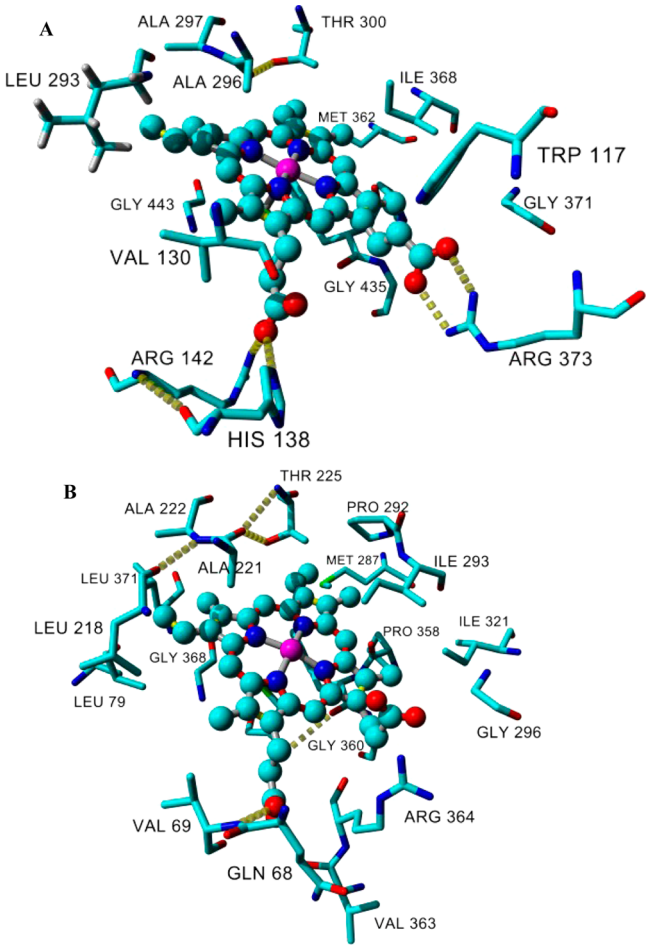

Figure 5. (A) Active site of full-length CYP26B1 after MD simulation. (B) Active site of spliced-CYP26B1 after MD simulation. Key amino acids interacting with the heme group are displayed in stick drawing. Hydrogen bonds are represented as yellow dashed lines.

template, is a good quality model and that it retains the heme moiety.

Ligand Docking into CYP26B1 Spliced Variant. Docking of atRA was performed in order to further evaluate the quality of the spliced-variant model. Our experimental results have shown that atRA binds to the spliced variant but that the catabolic rate for this isozyme is one-third of that observed for the full-length enzyme. No experimental information is to date available for other ligands.[23]

atRA was to this end docked in the active site of the CYP26B1 spliced variant, giving the C4 atom positioned 5.36 Å from the heme iron. The docked atRA does not interact through hydrogen bonding with any residue but presents multiple hydrophobic interactions with the amino acids Leu67, Gln68, Val69, Glu210, Arg213, Gly214, Glu217, Phe220, and Ala221 (Figure 4B). Such interactions hold the molecule within the active site, even though the binding energy is expected to be less strong than in the full-length enzyme.

The theoretically calculated binding energy for atRA is 91.10 kcal mol^{-1}, indicating that it still shows high affinity for the protein. The ~0.4 Å longer C4−Fe distance implies that it will be more difficult for the protein to react with the substrate in the spliced variant. The results are in agreement with experimental data,[23] showing that the spliced variant retains affinity for atRA but possesses a slower enzymatic activity compared to the full-length enzyme.

CONCLUSIONS

A new full-length homology model of CYP26B1 is presented, based on the cyanobacterial CYP120A1 template. Docking of atRA and a set of RAMBAs shows that the model convincingly discriminates between inducer (atRA), weak inhibitors, and strong inhibitors. On the basis of the full-length model, a homology model for the observed spliced variant of CYP26B1 was thereafter generated and analyzed. The spliced-variant homology model is concluded to be of high quality and retains the heme binding residues in essentially identical positions to the full-length form. The homology model of the spliced CYP26B1 is found to bind atRA at 4 times reduced affinity compared to the full-length version. The binding energy and position of the docked atRA suggests that this still binds to the enzyme variant and that the spliced variant retains the ability to catabolize atRA, although at reduced rate, in excellent agreement with experimental information showing 3-fold reduction in the rate of catabolism for the spliced variant.

A possible rationale for the existence of the spliced variant is that it regulates atRA degradation by reducing its availability and exhibiting slower catabolic rate than the full-length CYP26B1. This may prevent complete consumption of atRA in the cell after induction of CYP26B1. All computational results are in perfect agreement with recently described experimental information.

ASSOCIATED CONTENT

Supporting Information

Sequence alignment result and Ramachandran plot for the homology model of CYP26B1 spliced variant. This material is available free of charge via the Internet at http://pubs.acs.org.

AUTHOR INFORMATION

Corresponding Author

*E-mail: leif.eriksson@chem.gu.se.

Notes

The authors declare no competing financial interest.

ACKNOWLEDGMENTS

The Faculty of Science at the University of Gothenburg (LAE), the Faculty of Business, Science & Technology at Örebro University (ÅS), and the Facultad de Química, at UdelaR, Uruguay (PSM), are gratefully acknowledged for financial support.

REFERENCES

(1) Balmer, J. E.; Blomhoff, R. Gene expression regulation by retinoic acid. *J. Lipid Res.* **2002**, *43*, 1773−1808.
(2) Ross, A. C.; Zolfaghari, R.; Weisz, J. Vitamin A: recent advances in the biotransformation, transport, and metabolism of retinoids. *Curr. Opin. Gastroenterol.* **2001**, *17*, 184−192.
(3) Blomhoff, R.; Blomhoff, H. K. Overview of retinoid metabolism and function. *J. Neurobiol.* **2006**, *66*, 606−630.
(4) Zhao, Q.; Dobbs-Mc; E., L. Expression of CYP26B1 during zebrafish early development. *Gene Expression Patterns* **2005**, *5*, 363−369.
(5) Reijntjes, S.; Gale, E. Expression of the retinoic acid catabolising enzyme CYP26B1 in the chick embryo and its regulation by retinoic acid. *Gene Expression Patterns* **2003**, *3*, 621−627.
(6) Ray, W. J.; Bain, G.; Yao, M.; Gottlieb, D. I. CYP26, a novel mammalian cytochrome P450, is induced by retinoic acid and defines a new family. *J. Biol. Chem.* **1997**, *272*, 18702−18708.
(7) McSorley, L. C.; Daly, A. K. Identification of human cytochrome P450 isoforms that contribute to all-trans-retinoic acid 4-hydroxylation. *Biochem. Pharmacol.* **2000**, *60*, 517−526.
(8) Marill, J.; Cresteil, T.; Lanotte, M.; Chabot, G. G. Identification of human cytochrome P450s involved in the formation of all-trans-retinoic acid principal metabolites. *Mol. Pharmacol.* **2000**, *58*, 1341−1348.
(9) White, J. A.; Beckett-Jones, B.; Guo, Y. D.; Dilworth, F. J.; Bonasoro, J.; Jones, G.; Petkovich, M. cDNA cloning of human retinoic acid-metabolizing enzyme (hP450RAI) identifies a novel family of cytochromes P450. *J. Biol. Chem.* **1997**, *272*, 18538−18541.
(10) Pavez Lorié, E.; Li, H.; Vahlquist, A.; Törmä, H. The involvement of cytochrome P450 (CYP) 26 in the retinoic acid metabolism of human epidermal keratinocytes. *Biochim. Biophys. Acta* **2009**, *1791*, 220−228.
(11) Fujii, H.; Sato, T.; Kaneko, S.; Gotoh, O.; Fujii-Kuriyama, Y.; Osawa, K.; Kato, S.; Hamada, H. Metabolic inactivation of retinoic acid by a novel P450 differentially expressed in developing mouse embryos. *EMBO J.* **1997**, *16*, 4163−4173.
(12) Zolfaghari, R.; Cifelli, C. J.; Lieu, S. O.; Chen, Q.; Li, N.-q.; Ross, A. C. Lipopolysaccharide opposes the induction of CYP26A1 and CYP26B1 gene expression by retinoic acid in the rat liver in vivo. *Am. J. Physiol. Gastrointest. Liver Physiol.* **2007**, *292*, G1029−G1036.
(13) Mac Lean, G.; Abu-Abed. Cloning of a novel retinoic-acid metabolizing cytochrome P450, Cyp26B1, and comparative expression analysis with Cyp26A1 during early murine development. *Mech. Dev.* **2001**, *107*, 195−201.
(14) Topletz, A. R.; Thatcher, J. E.; Zelter, A.; Lutz, J. D.; Tay, S.; Nelson, W. L.; Isoherranen, N. Comparison of the function and expression of CYP26A1 and CYP26B1, the two retinoic acid hydroxylases. *Biochem. Pharmacol.* **2012**, *83*, 149−163.
(15) Taimi, M.; Helvig, C.; Wisniewski, J.; Ramshaw, H.; White, J.; Amad, M.; Korczak, B.; Petkovich, M. A novel human cytochrome P450, CYP26C1, involved in metabolism of 9-cis and all-trans isomers of retinoic acid. *J. Biol. Chem.* **2004**, *279*, 77−85.
(16) Gallagher, R. E. Retinoic acid resistance in acute promyelocytic leukemia. *Leukemia* **2002**, *16*, 1940−1958.
(17) Vanwauwe, J. P.; Coene, M. C.; Goossens, J.; Cools, W.; Monbaliu, J. Effects of cytochrome P-450 inhibitors on the in vivo metabolism of all-trans-retinoic acid in rats. *J. Pharmacol. Exp. Ther.* **1990**, *252*, 365−369.
(18) Kizaki, M.; Ueno, H.; Yamazoe, Y.; Shimada, M.; Takayama, N.; Muto, A.; Matsushita, H.; Nakajima, H.; Morikawa, M.; Koeffler, H. P.; Ikeda, Y. Mechanisms of retinoid resistance in leukemic cells: possible role of cytochrome P450 and P-glycoprotein. *Blood* **1996**, *87*, 725−733.
(19) Osanai, M.; Petkovich, M. Expression of the retinoic acid-metabolizing enzyme CYP26A1 limits programmed cell death. *Mol. Pharmacol.* **2005**, *67*, 1808−1817.
(20) Soppie, P.; Borgers, M.; Borghgraef, P.; Dillen, L.; Goossens, J.; Sanz, J.; Szel, H.; van Hove, C.; van Nyen, G.; Nobels, G.; Vanden Bossche, H.; Venet, M.; Willemsens, G.; Van Wauwe, J. P. R115866 inhibits all-trans-retinoic acid metabolism and exerts retinoidal effects in rodents. *J. Pharmacol. Exp. Ther.* **2000**, *293*, 304−312.
(21) Yamamoto, Y.; Zolfaghari, R.; Ross, A. C. Regulation of CYP26 (cytochrome P450RAI) mRNA expression and retinoic acid metabolism by retinoids and dietary vitamin A in liver of mice and rats. *FASEB J.* **2000**, *14*, 2119−2127.
(22) Nelson, D. R. A Second CYP26 P450 in Humans and Zebrafish: CYP26B1. *Arch. Biochem. Biophys.* **1999**, *371*, 345−347.
(23) Ateia Elmabsout, A.; Kumawat, A.; Saenz-Méndez, P.; Krivospitskaya, O.; Sävenstrand, H.; Olofsson, P. S.; Eriksson, L. A.; Strid, Å.; Valen, G.; Törmä, H.; Sirsjö, A. Cloning and Functional Studies of a Splice Variant of CYP26B1 Expressed in Vascular Cells. *PLoS ONE* **2012**, *7*, e36839.
(24) Krieger, E.; Nabuurs, S. B.; Vriend, G. Homology Modeling. In *Structural Bioinformatics*; Bourne, P. E., Weissig, H., Eds.; Wiley-Liss, Inc.: Hoboken, NJ, 2003; Vol. *44*, pp 507−521.
(25) Gomaa, M. S.; Yee, S. W.; Milbourne, C. E.; Barbera, M. C.; Simons, C.; Brancale, A. Homology model of human retinoic acid metabolising enzyme cytochrome P450 26A1 (CYP26A1): Active site architecture and ligand binding. *J. Enzyme Inhib. Med. Chem.* **2006**, *21*, 361−369.
(26) Karlsson, M.; Strid, Å.; Sirsjö, A.; Eriksson, L. A. Homology Models and Molecular Modeling of Human Retinoic Acid Metabolizing Enzymes Cytochrome P450 26A1 (CYP26A1) and P450 26B1 (CYP26B1). *J. Chem. Theory Comput.* **2008**, *4*, 1021−1027.
(27) Krieger, E. Yet Another Scientific Artificial Reality Application (YASARA), 2004.
(28) Krieger, E.; Joo, K.; Lee, J.; Lee, J.; Raman, S.; Thompson, J.; Tyka, M.; Baker, D.; Karplus, K. Improving physical realism, stereochemistry, and side-chain accuracy in homology modeling: Four approaches that performed well in CASP8. *Proteins* **2009**, *77*, 114−122.
(29) Duan, Y.; Wu, C.; Chowdhury, S.; Lee, M. C.; Xiong, G.; Zhang, W.; Yang, R.; Cieplak, P.; Luo, R.; Lee, T.; Caldwell, J.; Wang, J.; Kollman, P. A Point-Charge Force Field for Molecular Mechanics Simulations of Proteins Based on Condensed-Phase Quantum Mechanical Calculations. *J. Comput. Chem.* **2003**, *24*, 1999−2012.
(30) Essmann, U.; Perera, L.; Berkowitz, M. L.; Darden, T.; Lee, H.; Pedersen, L. G. A smooth particle mesh Ewald method. *J. Chem. Phys.* **1995**, *103*, 8577−8593.
(31) Altschul, S. F.; Madden, T. L.; Schäffer, A. A.; Zhang, J.; Zhang, Z.; Miller, W.; Lipman, D. J. Gapped BLAST and PSI-BLAST: a new generation of protein database search programs. *Nucleic Acids Res.* **1997**, *25*, 3389−3402.
(32) Kühnel, K.; Ke, N.; Cryle, M. J.; Sligar, S. G.; Schuler, M. A.; Schlichting, I. Crystal Structures of Substrate-Free and Retinoic Acid-Bound Cyanobacterial Cytochrome P450 CYP120A1. *Biochemistry* **2008**, *47*, 6552−6559.
(33) Surendhar Reddy, C.; Vijayasarathy, K.; Srinivas, E.; Madhavi Sastry, G.; Narahari Sastry, G. Homology modeling of membrane proteins: A critical assessment. *Comput. Biol. Chem.* **2006**, *30*, 120−126.
(34) Xiang, Z. Advances in Homology Protein Structure Modeling. *Curr. Protein Pept. Sci.* **2006**, *7*, 217−227.
(35) Kirton, S. B.; Baxter, C. A.; Sutcliffe, M. J. Comparative modeling of cytochromes P450. *Adv. Drug Delivery Rev.* **2002**, *54*, 385−406.
(36) Laskowski, R. A.; MacArthur, M. W.; Moss, D. S.; Thornton, J. M. PROCHECK - a program to check the stereochemical quality of protein structures. *J. Appl. Crystallogr.* **1993**, *26*, 283−291.
(37) Bowie, J. U.; Lüthy, R.; Eisenberg, D. A method to identify protein sequences that fold into a known three-dimensional structure. *Science* **1991**, *253*, 164−170.
(38) RAMPAGE server: http://mordred.bioc.cam.ac.uk/~rapper/rampage.php.
(39) Morris, G. M.; Goodsell, D. S.; Halliday, R. S.; Huey, R.; Hart, W. E.; Belew, R. K.; Olson, A. J. Automated Docking Using a Lamarckian Genetic Algorithm and an Empirical Binding Free Energy Function. *J. Comput. Chem.* **1998**, *19*, 1639−1662.

(40) Pontius, J.; Richelle, J.; Wodak, S. J. Deviations from Standard Atomic Volumes as a Quality Measure for Protein Crystal Structures. *J. Mol. Biol.* **1996**, *264*, 121−136.
(41) Bujnicki, J.; Rychlewski, L.; Fischer, D. Fold-recognition detects an error in the Protein Data Bank. *Bioinf. Discovery* **2002**, *18*, 1391−1395.
(42) Yee, S. W.; Jarno, L.; Gomaa, M. S.; Elford, C.; Ooi, L. L.; Coogan, M. P.; McClelland, R.; Nicholson, R. I.; Evans, B. A. J.; Brancale, A.; Simons, C. Novel tetralone-derived retinoic acid metabolism blocking agents: Synthesis and in vitro evaluation with liver microsomal and MCF-7 CYP26A1 cell assays. *J. Med. Chem.* **2005**, *48*, 7123−7131.
(43) White, J. A.; Ramshaw, H.; Taimi, M.; Stangle, W.; Zhang, A.; Everingham, S.; Creighton, S.; Tam, S.-P.; Jones, G.; Petkovich, M. Identification of the human cytochrome P450, P450RAI-2, which is predominantly expressed in the adult cerebellum and is responsible for all-trans-retinoic acid metabolism. *Proc. Natl. Acad. Sci. U.S.A.* **2000**, *97*, 6403−6408.